1229207

15032410038

Acrobat 8.0

# CALCULATION COVER SHEET

Project Title: 300 Area Closure Operations **Job No. 14655**

Area: 300 Area

Discipline: Nuclear/Safety Engineering *Calculation No: 0300X-CA-N0140

Subject: Characterization of the Soil Contamination Under 324 B Cell

Computer Program: MCNP 5, ORIGEN 2.2, Radcalc 4.1 Program No: NA

The attached calculations have been generated for a specific purpose and task. Use of the calculations by persons who do not have access to all pertinent facts may lead to incorrect conclusions and/or results. Before applying these calculations to your work, the underlying basis, rationale, and other pertinent information relevant to these calculations must be thoroughly reviewed with appropriate Washington Closure Hanford LLC (WCH) officials or other authorized personnel. WCH is not responsible for the use of a calculation not under its direct control.

Committed Calculation ☒ Preliminary ☐ Superseded ☐ Voided ☐

| Rev. | Sheet Numbers | Originator | Checker | Reviewer | Approval | Date |
|---|---|---|---|---|---|---|
| 2 | 1-24 | W. Josephson | R. Reeder | NA | S. Marske | |
| | Attachment A, 1-38 | | | | | 02.19.15 |
| | Attachment B, 1-56 | 02/18/15 | 2/19/15 | | | |
| | Attachment C, 1-436 | | | | | |
| | Attachment D, 1-1 | | | | | |
| | Attachment E, 1-4 | | | | | |
| | | | | | | |

## SUMMARY OF REVISION

| | |
|---|---|
| 0 | Initial issue |
| 1 | Added modeling for the range of measured soil densities |
| 2 | Incorporated new penetrometer measurements |

RECEIVED MAR 24 2015 EDMC

Washington Closure
Hanford LLC

# CALCULATION SHEET

| | | | | | | | |
|---|---|---|---|---|---|---|---|
| **Originator** | W. Josephson | **Date** | 02/18/15 | **Calc. No.** | 0300X-CA-N0140 | **Rev. No.** | 2 |
| **Project** | 300 Area Closure Operations | **Job No.** | 14655 | **Checked** | R. Reeder | **Date** | 02/18/15 |
| **Subject** | Characterization of the Soil Contamination Under 324 B Cell | | | | | **Sheet No.** | 1 of 24 |

## Table of Contents


1.0 Purpose ..... 3
2.0 Methodology ..... 3
2.1 Penetrometer Activities ..... 3
2.2 Soil Contamination Plume ..... 4
3.0 Exposure Rate to Activity Calculations ..... 4
3.1 Physical Constants ..... 4
3.2 Elemental Masses ..... 4
3.3 Penetrometer Survey Data ..... 6
3.4 Isotopic Distribution ..... 8
3.5 Photon Source per Curie ..... 10
3.6 Material Compositions ..... 12
3.7 Tally Conversion Factor ..... 12
3.8 MCNP Models ..... 14
3.9 Solvers ..... 15
4.0 Contamination Plume Calculations ..... 19
4.1 Activity Distribution ..... 19
4.2 Activity Profile ..... 20
4.3 Total Activity ..... 21
4.4 Actinide Activity ..... 21
4.5 Decay Heat ..... 22
4.6 Uncertainty Analysis ..... 23
5.0 References ..... 24

Attachment A: Penetrometer Survey Measurements
Attachment B: ORIGEN Output Files
Attachment C: MCNP Output Files
Attachment D: Source Volume Activities
Attachment E: Radcalc Output Files


## Tables


Table 1. Physical Constants ..... 4
Table 2. Atomic Masses and Abundances ..... 5
Table 3. Elemental Masses ..... 6
Table 4: Penetrometer Summary ..... 6
Table 5: Radiological Survey Record Summary ..... 7
Table 6. 324 B Cell Timeline ..... 9
Table 7. FRG Glass Log Summary ..... 10
Table 8. Photon Rates ..... 11
Table 9: MCNP Materials Summary ..... 12
Table 10. Formula Mass of Air ..... 14
Table 11: Penetrometer Activities ..... 16
Table 12: Penetrometer Activity Comparison ..... 16

Table 13: Population Statistics ..... 19
Table 14. Contamination Zone Volumes ..... 21
Table 15. Contaminated Soil Activities ..... 21
Table 16. Plutonium Activities ..... 22
Table 17. Decay Heat ..... 22

## Figures

Figure 1. Photon Spectrum ..... 11
Figure 2. MCNP Model ..... 15
Figure 3: Solution Quality ..... 17
Figure 4. Activity Distributions ..... 19
Figure 5. Activity Profile ..... 20

## Acronyms

| | |
|---|---|
| AMDC | Atomic Mass Data Center |
| DWVP | Defense Waste Vitrification Project |
| FRG | Federal Republic of Germany |
| GRG | Generalized Reduced Gradient |
| HHU | Hydraulic Hammer Unit |
| LANL | Los Alamos National Laboratory |
| MCNP | Monte Carlo N-Particle |
| NWTP | Nuclear Waste Treatment Project |
| NWVP | Nuclear Waste Vitrification Project |
| ORIGEN | Oak Ridge Isotope Generation and Depletion |
| PNNL | Pacific Northwest National Laboratory |
| RLFCM | Radioactive Liquid-Fed Ceramic Melter |
| TMI | Three-Mile Island |
| TRU | Transuranic waste as defined in DOE M435.1-1 |
| WESF | Waste Encapsulation and Storage Facility |
| WSEP | Waste Solidification Engineering Prototypes |

## 1.0 Purpose

An effort to characterize the magnitude and extent of the soil contamination plume under the 324 B Cell (300-296 waste site) has been on-going for several years. As part of this effort, a series of penetrometers were driven beneath the cell, and exposure rates along the penetrometers were measured using field exposure rate instruments of various ranges. The measured exposure rates indicate that a high level of soil contamination is present underneath 324 B Cell. The intent of this calculation is to utilize the field exposure rate measurements to calculate the activity concentrations and total activities in the contamination plume.

## 2.0 Methodology

This calculation proceeded in two distinct phases. First, the activities associated with the individual penetrometers were determined using exposure rate to activity methods. Then the penetrometer results were extended to characterize the entire soil contamination plume. The methodology associated with each phase is discussed in greater detail in the subsequent sections.

### 2.1 Penetrometer Activities

The activity associated with each penetrometer was determined using exposure rate measurements along the length of the housing and exposure rate to activity conversion factors. This approach is often referred to as a "dose to curie" or "dose rate to curie" methodology, although the use of the term "dose" in this context is erroneous.

Exposure rate to curie conversion factors were calculated using version 5.160 of the Monte-Carlo N Particle (MCNP) code developed by the Los Alamos National Laboratory (LANL 2008). A series of three-dimensional MCNP models of the penetrometers were developed, including the steel pipes, cone penetrator, soil surrounding the pipes, and the locations of all exposure rate measurements.

The composition of the radioactive material was determined from an examination of the timeline of activities performed in the 324 B Cell. A single release of concentrated Cs-137 and Sr-90 activity appeared to be the only source of sufficient radioactive material to produce the measured exposure rates.

The photon spectrum given off by the radioactive material was calculated using version 2.2 of the Oak Ridge Isotope Generation and Depletion (ORIGEN) code developed by the Oak Ridge National Laboratory (ORNL 1980). The photon spectrum was incorporated into the MCNP models directly. Once complete, the MCNP models were executed to calculate the required exposure rate to curie conversion factors.

The exposure rate to curie conversion factors, assumed source activities, and measured exposure rates were entered into a series of Microsoft Excel workbooks, one for each penetrometer. A matrix equation was assembled in each workbook to calculate exposure rates based on the assumed source activities, and a quality metric was formed using the sum of the relative exposure rate errors. The iterative solver built into Microsoft Excel was then used to adjust the assumed source activities to minimize the quality metric.

## 2.2 Soil Contamination Plume

The results from the individual penetrometers were extended to generate an approximation of the three-dimensional contamination plume. The contamination plume was assumed to include three zones which follow the path of the expansion joint in the floor of the cell. The radioactive material was assumed to have propagated downward to the cobble layer 4 feet beneath the footers of the hot cell, and to spread horizontally with increasing depth. The concentrations of activity in each zone were based on averages from the individual Geoprobe results. The sum of the zone volumes times the zone concentrations yield the total activity of the contamination plume.

## 3.0 Exposure Rate to Activity Calculations

The soil contamination activities corresponding to the penetrometer exposure rates are calculated in the following sections.

## 3.1 Physical Constants

Physical constants are used in a number of steps to perform calculations and convert units. The physical constants used are listed in Table 1.

**Table 1. Physical Constants**

| Name | Symbol | Value | Units | Reference |
|---|---|---|---|---|
| Atomic Mass Constant | $m_uc^2$ | 931.494028 | MeV-mole/gm | CODATA 2006 |
| Average Energy to Produce an Ion Pair | W | 33.8 | eV/e | ICRU 1979 |
| Avogadro Constant | $N_{av}$ | 6.02214179E+23 | atoms/mole | CODATA 2006 |
| Barn | b | 1.0E-24 | $cm^2$ | NIST 2008 |
| Curie | Ci | 3.7E+10 | decays/s | NIST 2008 |
| Electron Volt | eV | 1.602176487E-19 | J | CODATA 2006 |
| Electron Charge | e | 1.602176487E-19 | C | CODATA 2006 |
| Electrostatic Unit | esu | 3.335641E-10 | C | NIST 2008 |
| Roentgen | R | 2.58E-04 | C/kg | NIST 2008 |

## 3.2 Elemental Masses

Elemental masses were calculated from atomic masses and abundances. Atomic masses and abundances were taken from the NUBASE 2003 evaluation published by the Atomic Mass Data Center (AMDC 2003). The raw data was first downloaded as a text file called nubtab03.txt. The text information was copied and pasted into a Microsoft Excel workbook called NUBASE2003.xlsx for further processing.

Atomic masses in AMDC 2003 are stated in terms of mass excess, which is the difference between the atomic mass number and the actual atomic mass. Mass excess values in AMDC 2003 are stated in terms of equivalent energy in MeV. Mass excess values may be positive or negative depending on the isotope. Mass excess values were converted to atomic masses using the atomic mass constant in Section 3.1 and the equation below.

$$AM_i = AN_i + \left( \frac{ME_i}{931.494028\ \text{MeV} \cdot \text{mole/g}} \right)$$

In the above equation, AM is the atomic mass, AN is the atomic mass number, and ME is the mass excess. The subscript i refers to individual isotopes. The calculated atomic masses were rounded to eight significant figures. The atomic masses and abundances used in this calculation are listed in Table 2.

**Table 2. Atomic Masses and Abundances**

| Isotope | Atomic Mass (gm/mole) | Abundance | Isotope | Atomic Mass (gm/mole) | Abundance |
|---|---|---|---|---|---|
| C-12 | 12.000000 | 0.9893 | Cr-54 | 53.938880 | 0.02365 |
| C-13 | 13.003355 | 0.0107 | Mn-55 | 54.938045 | 1 |
| N-14 | 14.003074 | 0.99632 | Fe-54 | 53.939610 | 0.05845 |
| N-15 | 15.000109 | 0.00368 | Fe-56 | 55.934937 | 0.91754 |
| O-16 | 15.994915 | 0.99757 | Fe-57 | 56.935394 | 0.02119 |
| O-17 | 16.999132 | 0.00038 | Fe-58 | 57.933276 | 0.00282 |
| O-18 | 17.999161 | 0.00205 | Ni-58 | 57.935343 | 0.680769 |
| Si-28 | 27.976927 | 0.922297 | Ni-60 | 59.930786 | 0.262231 |
| Si-29 | 28.976495 | 0.046832 | Ni-61 | 60.931056 | 0.011399 |
| Si-30 | 29.973770 | 0.030872 | Mo-92 | 91.906811 | 0.1484 |
| Ar-36 | 35.967545 | 0.003365 | Mo-94 | 93.905088 | 0.0925 |
| Ar-38 | 37.962732 | 0.000632 | Mo-95 | 94.905842 | 0.1592 |
| Ar-40 | 39.962383 | 0.996003 | Mo-96 | 95.904679 | 0.1668 |
| Cr-50 | 49.946044 | 0.04345 | Mo-97 | 96.906022 | 0.0955 |
| Cr-52 | 51.940508 | 0.83789 | Mo-98 | 97.905408 | 0.2413 |
| Cr-53 | 52.940649 | 0.09501 | Mo-100 | 99.907478 | 0.0963 |

Elemental masses were calculated using the atomic mass and abundance values in Table 2. The equation for elemental mass calculations is given below:

$$EM = \sum_i AM_i \cdot AB_i$$

In the above equation, EM is the elemental mass, AM is the atomic mass, and AB is the abundance. The subscript i refers to individual isotopes. The subtotaling feature in Microsoft Excel was used to complete the elemental mass calculations. The calculated elemental masses were rounded to eight significant figures. The elemental masses used in this calculation are listed in Table 3.

**Table 3. Elemental Masses**

| Element | Elemental Mass (gm/mole) | Element | Elemental Mass (gm/mole) |
|---|---|---|---|
| C | 12.010736 | Cr | 51.996133 |
| N | 14.006743 | Mn | 54.938045 |
| O | 15.999405 | Fe | 55.845145 |
| Si | 28.085413 | Ni | 58.693352 |
| Ar | 39.947677 | Mo | 95.931292 |

### 3.3 Penetrometer Survey Data

Survey data under 324 B Cell has been obtained by driving penetrometers through the soil, and extending instruments down the penetrometers to record exposure rate as a function of distance. The penetrometers driven to date are summarized in Table 4.

**Table 4: Penetrometer Summary**

| Cap ID | Driving Unit | Orientation | Length |
|---|---|---|---|
| C8207 | Geoprobe | Horizontal | 65 ft |
| C8208 | Geoprobe | Horizontal | 65 ft |
| C8209 | Geoprobe | Horizontal | 65 ft |
| C8210 | Geoprobe | Horizontal | 80 ft |
| C8211 | Geoprobe | Horizontal | 70 ft |
| C8212 | Geoprobe | Horizontal | 70 ft |
| C8213 | Geoprobe | Horizontal | 75 ft |
| C8214 | Geoprobe | Horizontal | 80 ft |
| C8215 | HHU | Angled | 89 ft |
| C8216 | HHU | Angled | 105 ft |
| C9433 | Geoprobe | Horizontal | 60 ft |
| C9434 | Geoprobe | Horizontal | 75 ft |
| C9435 | Geoprobe | Horizontal | 75 ft |
| C9436 | Geoprobe | Horizontal | 70 ft |
| C9437 | Geoprobe | Horizontal | 95 ft |
| C9438 | Geoprobe | Horizontal | 85 ft |

Exposure rates were recorded at least every foot, and more frequently in regions exhibiting rapid change or peaking in the exposure rate profile. The exposure rate data is recorded in the Radiological Survey Record (RSR) documents shown in Table 5.

**Table 5: Radiological Survey Record Summary**

| RSR Number | Date | Instrument | Penetrometers Surveyed |
|---|---|---|---|
| 300PS-10-3851 | 11/09/10 | RO-7 Low/Mid/High | Penetrometer refused, abandoned in place |
| 300PS-10-3889 | 11/10/10 | RO-7 Low/Mid/High | C8207 |
| 300PS-10-3904 | 11/12/10 | RO-7 Low/Mid/High | C8208 |
| 300PS-10-3963 | 11/16/10 | RO-7 Low/Mid/High | C8209, C8210 |
| 300PS-10-3996 | 11/17/10 | RO-7 Low/Mid/High | C8211, C8212 |
| 300PS-10-4025 | 11/18/10 | RO-7 Low/Mid/High | C8213, C8214 |
| 300PS-11-1990 | 05/03/11 | AMP-50 | C8215, C8216 |
| 300PS-14-0530 | 09/29/14 | AMP-50/100/200 | C9433, C9434, C9435 |
| 300PS-14-0538 | 10/01/14 | AMP-50/100/200 | C8207, C8208, C8209, C8210, C8211 |
| 300PS-14-0547 | 10/02/14 | AMP-50/100/200 | C9436 |
| 300PS-14-0556 | 10/06/14 | AMP-50 | C9437 |
| 300PS-14-0557 | 10/06/14 | AMP-50/100/200 | C8212, C8213 |
| 300PS-14-0561 | 10/07/14 | AMP-50/100/200 | C8214 |
| 300PS-14-0573 | 10/09/14 | AMP-50/100/200 | C9438 |
| 300PS-14-0616 | 10/23/14 | AMP-50 | C8216 |
| 300PS-14-0627 | 10/28/14 | AMP-50 | C8215 |

For the purposes of this calculation, the exposure rates recorded in 2010 and 2011 were ignored for the following reasons:

- **Instrument Consistency**: All of the measurements taken in 2010 and 2011 were recorded using RO-7 series instruments. These measurements were also taken in 2014 using AMP series instruments. Additional penetrometers driven since 2011 were also surveyed in 2014 using AMP series instruments. To ensure a valid comparison, all activities in this calculation were based on measurements collected with AMP series instruments.

- **Distance Uncertainty**: In order to drive newer penetrometers, the ends of existing penetrometers occasionally had to be removed. As work progressed, configuration control was lost on some of the earlier penetrometers, introducing uncertainty in the locations of the exposure rate measurements. All of the earlier exposure rate measurements were repeated in part to ensure the measurements included validated distance information.

- **Changing Conditions**: Another reasons for repeating the earlier exposure rate measurements was to evaluate any changes in the exposure rate profiles over time. Although most of the current exposure rate profiles were quite similar to the original measurements, there were some that exhibited significant variations. The 2014 measurements were used exclusively to ensure that the calculated activities reflected current conditions as closely as possible.

The hydraulic hammer unit (HHU) penetrometers were driven at an angle to evaluate the vertical profile deep below the 324 Facility. Since these penetrometers were not intended to assess the high activity plume directly beneath 324 B Cell, they were also ignored in this calculation.
In many cases, the exposure rate at specific penetrometer locations were recorded using more than one

range of instrument. In cases where more than one measurement existed, the value obtained with the lowest range instrument was considered the most accurate, and was used for all subsequent calculations.

Penetrometer survey measurements are summarized in Attachment A.

### 3.4 Isotopic Distribution

Given the measured exposure rates discussed in Section 3.3, the soil contamination under 324 B Cell represents tens of thousands of curies. To help identify the possible sources of this quantity of radioactive material, and the isotopic composition of the possible sources, an operational timeline for 324 B Cell was constructed. The major projects conducted are shown in Table 6.

The soil contamination may have been associated with a single, large release or a series of smaller releases over time. The only known release of sufficient magnitude was a single spill of concentrated radioactive liquid during the Federal Republic of Germany (FRG) Canister Fabrication Project, known locally as the FRG glass log project. The spill is described in two places in HNF-2750 (BWHC 1998). The accounts differ in terms of the activities released as shown below.

> The largest of these spills accounts for most of the estimated dispersible radioactivity within B-Cell. This spill, which took place in October 1986, resulted in an estimated 1271 kCi (883 kCi Cs-137 and 338 kCi Sr-90) being released to the cell. (HNF-2750, Section 2.1.1.1)
>
> During routine transfers of radioactive material on October 21, 1986, for the FRG Canister Fabrication Project, approximately 510 liters of concentrated Cs-137/Sr-90 solution leaked to the floor of B-Cell. The estimated radiochemical inventory of the solution was 883 kCi Cs-137 and 388 kCi Sr-90. (HNF-2750, Section 2.1.1.3)

For the purposes of this calculation, the total activity released was interpreted as 1271 kCi, which is the sum of 883 kCi of Cs-137 and 388 kCi of Sr-90.

**Table 6. 324 B Cell Timeline**

| Project | Description | Dates | Refs |
|---|---|---|---|
| WSEP | One of the initial missions of the 324 Facility. Evaluated pot solidification, spray solidification, and phosphate glass vitrification technologies. Used PUREX 1WW or B Plant fission product streams as feed. | 1966-1968 | BNWL-1667 |
| NWVP | This project was intended to test the most promising technology from WSEP. Commercial LWR fuel from Point Beach reactor sheared and dissolved in B Cell, liquid piped to 325A for PUREX reprocessing, fission product stream piped back to B Cell for vitrification. | 1976-1979 | PNL-3038 |
| DWVP | This project was intended to test the effectiveness of vitrification technologies on high-level defense waste. The processes tested included a spray calciner/in-can melter, spray calciner/ceramic melter and direct liquid feeding of a ceramic melter. Used simulated Hanford tank waste as feed. | 1980 | PNL-3818 |
| TMI Resins | Spent resins from Three-Mile Island were solidified, encapsulated, and packaged. | Early 1980s | WHC-MR-0388 |
| NWTP | PNNL developed and tested the Radioactive Liquid-Fed Ceramic Melter (RLFCM) as part of NWTP efforts toward treating commercial nuclear power related waste. | 1982-1986 | PNL-5470 |
| FRG Glass Logs | FRG contracted DOE to make heat and radiation sources to test a repository proposal in the Asse salt mine. PNL concentrated Cs and Sr streams from B Plant to obtain the desired loading, and vitrified the waste in B Cell using the RLFCM. FRG was not able to obtain licensing for the proposed repository, and did not take possession of the glass logs. A 510L leak from this campaign, estimated at 883 KCi Cs-137 and 388 KCi Sr-90, took place on Oct 21, 1986. | 1986-1987 | HNF-2570<br>PNL-6790<br>PNL-SA-15147 |

The intent of the FRG Canister Fabrication Project was to fabricate radiation and heat sources comparable to spent reactor fuel, but without the actinide content and long-term degradation issues associated with spent reactor fuel. The sources utilized a borosilicate glass matrix loaded with Cs-137 to provide the required radiation and with Sr-90 to provide the required decay heat. The Cs-137 material came from 187 capsules from the Waste Encapsulation and Storage Facility (WESF), which were cut open specifically for that effort. The Sr-90 came from unused WESF feed solutions remaining in tank heels in B Plant. For purposes of comparison, the average content of the FRG glass logs by run was extracted from WSR-20A-00 (BWHC 1997) and is summarized in Table 7.

**Table 7. FRG Glass Log Summary**

| Run | Average Properties | | | |
|---|---|---|---|---|
| | Cs-137 Activity (kCi) | Sr-90 Activity (kCi) | Decay Heat (W) | Surface Exposure Rate (R/hr) |
| RLFCM-7 | 192 | 85 | 1490 | 272,000 |
| RLFCM-8 | 78 | 143 | 1330 | 112,000 |
| RLFCM-9 | 207 | 130 | 1860 | 310,000 |
| RLFCM-10 | 136 | 59 | 1047 | 210,000 |

As shown in Table 7, the spill constituted sufficient material for approximately four of the highest activity logs. Some of the spilled material was recovered during cell cleaning. The remaining material remained unaccounted for.

### 3.5 Photon Source per Curie

As discussed in Section 3.4, the most likely source of the contamination underneath 324 B Cell was the spill of concentrated feed solution during the Federal Republic of Germany (FRG) Canister Fabrication Project. The estimated radiochemical inventory of the solution was 883 kCi Cs-137 and 388 kCi Sr-90, along with small concentrations of actinide contaminants.

The photon rate and spectrum from a curie of this material was calculated using version 2.2 of the Oak Ridge Isotope Generation (ORIGEN) code (ORNL 1980). Separate input files were generated with one gram of Cs-137 and one gram of Sr-90. Both input files were provided with a one year decay time to allow the daughter radionuclides to reach equilibrium. The cases were then executed using the photon library for water provided with ORIGEN. All ORIGEN runs were performed by URS Princeton using validation code and compters. The ORIGEN outputs are included as Attachment B.

The photon spectrum from each ORIGEN run was divided by the activity of the parent isotope at the end of the decay period to form photon rates and spectra per curie. The photon rates and spectra were then combined using the activity ratio present in the FRG Canister Fabrication project spill.

It is well known that the energy bin structure used by ORIGEN under-predicts the exposure rate associated with Cs-137 due to the mismatch between the center energy of the bin (575 keV) and the energy of the Cs-137 decay photon (662 keV). Therefore the bin energy of both spectra was raised to 662 keV, and the number of photons in the bin was reduced by a factor of 575/662 to maintain a uniform

energy rate. The results are shown in Table 8 and Figure 1.

**Table 8. Photon Rates**

| Avg Energy (MeV) | Photon Rate (γ/sec/Ci) | | | Fractional Spectrum |
|---|---|---|---|---|
| | Cs-137 | Sr-90 | Combined | |
| 1.00E-02 | 4.629E+08 | 2.215E+09 | 9.977E+08 | 3.968E-02 |
| 2.50E-02 | 5.733E+07 | 4.745E+08 | 1.847E+08 | 7.345E-03 |
| 3.75E-02 | 2.313E+09 | 3.157E+08 | 1.703E+09 | 6.775E-02 |
| 5.75E-02 | 4.550E+07 | 4.619E+08 | 1.726E+08 | 6.866E-03 |
| 8.50E-02 | 2.300E+07 | 2.880E+08 | 1.039E+08 | 4.132E-03 |
| 1.25E-01 | 1.236E+07 | 1.929E+08 | 6.749E+07 | 2.684E-03 |
| 2.25E-01 | 1.051E+07 | 2.726E+08 | 9.051E+07 | 3.600E-03 |
| 3.75E-01 | 1.861E+06 | 1.296E+08 | 4.085E+07 | 1.625E-03 |
| 6.62E-01 [1] | 3.131E+10 | 6.495E+07 | 2.177E+10 | 8.660E-01 |
| 8.50E-01 | 3.959E+04 | 2.669E+07 | 8.175E+06 | 3.251E-04 |
| 1.25E+00 | 2.623E+02 | 1.081E+07 | 3.300E+06 | 1.313E-04 |
| 1.75E+00 | 0.000E+00 | 1.221E+06 | 3.729E+05 | 1.483E-05 |
| 2.25E+00 | 0.000E+00 | 2.920E+02 | 8.915E+01 | 3.546E-09 |
| 2.75E+00 | 0.000E+00 | 0.000E+00 | 0.000E+00 | 0.000E+00 |
| 3.50E+00 | 0.000E+00 | 0.000E+00 | 0.000E+00 | 0.000E+00 |
| 5.00E+00 | 0.000E+00 | 0.000E+00 | 0.000E+00 | 0.000E+00 |
| 7.00E+00 | 0.000E+00 | 0.000E+00 | 0.000E+00 | 0.000E+00 |
| 9.50E+00 | 0.000E+00 | 0.000E+00 | 0.000E+00 | 0.000E+00 |
| Total | 3.424E+10 | 4.454E+09 | 2.514E+10 | 1.000E+00 |

Note 1 Average energy and photon rate adjusted to account for Cs-137 contribution

**Figure 1. Photon Spectrum**

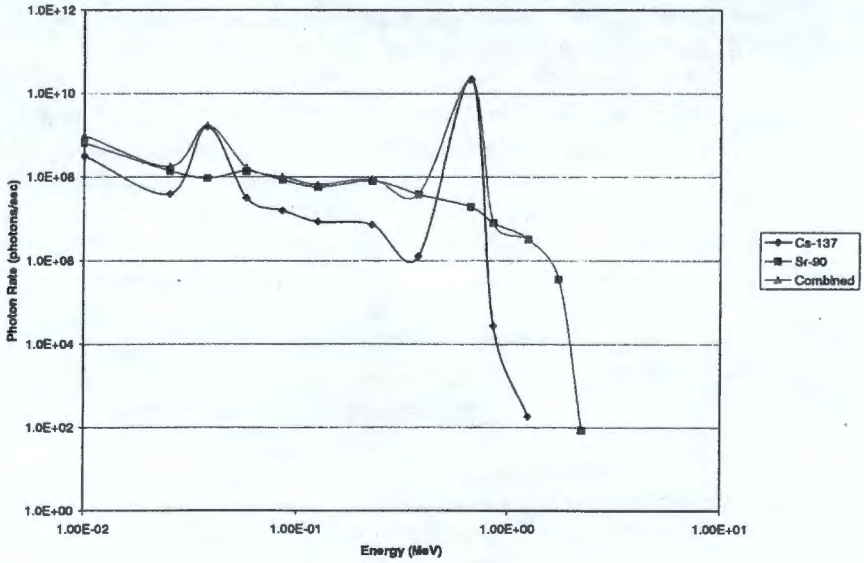

### 3.6 Material Compositions

The MCNP models include the carbon steel penetrometers, the air inside the penetrometers, and the soil column surrounding the penetrometers. Material compositions and densities were taken from PNNL-15870, Revision 1 (PNNL 2011), with the following exceptions.

- Since PNNL-15870 does not include a soil composition, Hanford soil was assumed to have the same composition as granite (mat 267). The nominal density of Hanford soil was taken to be 1.67 grams per cubic centimeter as documented in ANS 1992.

- The Roentgen is currently defined as a deposition of charge of both signs by ionizing radiation of 2.58E-04 coulombs per kilogram in dry air at standard temperature (15 °C) and pressure (1 atm). Historically, the Roentgen was defined as the deposition of one electrostatic unit of charge of either sign by ionizing radiation in a cubic centimeter of dry air at standard temperature and pressure. These two definitions of the Roentgen imply an air density given by the equation below.

$$\left(\frac{3.335641\cdot 10^{-10}\ \mathrm{C}}{\mathrm{cm}^3}\right)\cdot\left(\frac{\mathrm{kg}}{2.58\cdot 10^{-4}\ \mathrm{C}}\right)=1.29\cdot 10^{-3}\ \frac{\mathrm{g}}{\mathrm{cm}^3}$$

  To ensure consistency with the tally conversion factor in Section 3.7, the air density above was used instead of the air density in PNL-15870.

The materials in the MCNP input files are summarized in Table 9.

**Table 9: MCNP Materials Summary**

| MCNP Material | Where Used | PNNL-15870 Composition | Density (g/mL) |
|---|---|---|---|
| Carbon Steel | Penetrometers | Mat 294 | 7.82000 |
| Air | Air inside penetrometers | Mat 4 | 0.00129 |
| Soil | Soil Column | Mat 267 | 1.67000 |

### 3.7 Tally Conversion Factor

A standard MCNP tally calculates the average particle fluence over a cell, over a surface, or at a point, and is reported in units of particle fluence, or particles per square centimeter per particle history. Particle fluence may be converted to other quantities of interest using conversion factors and reaction cross-sections. In MCNP, tallies are multiplied by conversion factors and cross-sections using the FM card.

A tally (T) may be multiplied by the number of particle histories per unit time to convert from a per history basis to a per unit time basis. This may be done using the FM card, or by starting each particle with a weight value (WGT) equal to the particle rate per unit time. It is convenient to use the WGT parameter for this conversion because it is problem dependent, while most other conversion factors are problem independent.

$$T \cdot WGT = \left(\frac{\text{particles}}{\text{cm}^2 \cdot \text{history}}\right) \cdot \left(\frac{\text{histories}}{\text{sec}}\right) = \frac{\text{particles}}{\text{cm}^2 \cdot \text{sec}}$$

A tally may be multiplied by the energy-dependent total reaction cross-section ($\sigma_t$) to convert to total reaction rate. Cross-sections in MCNP are microscopic quantities, and are recorded in units of barns. To obtain the macroscopic reaction rate in a material, the tally must also be multiplied by the atom density of the material ($\rho_a$). In MCNP, atom densities are expressed in units of barn-centimeters to simplify the multiplication.

$$T \cdot WGT \cdot \sigma_t \cdot \rho_a = \left(\frac{\text{particles}}{\text{cm}^2 \cdot \text{history}}\right) \cdot \left(\frac{\text{histories}}{\text{sec}}\right) \cdot (\text{b}) \cdot \left(\frac{\text{atoms}}{\text{b} \cdot \text{cm}}\right) = \frac{\text{reactions}}{\text{cm}^3 \cdot \text{sec}}$$

A reaction rate may be multiplied by the energy-dependent heating cross-section ($\sigma_h$) to convert to energy absorbed. Heating cross-sections are stated in units of MeV per collision. Since dosimetric quantities are stated in terms of energy absorbed per gram of material, the reaction rate may also be divided by the mass density ($\rho_m$) of the material in grams per cubic centimeter.

$$T \cdot WGT \cdot \sigma_t \cdot \sigma_h \cdot \left(\frac{\rho_a}{\rho_m}\right) = \left(\frac{\text{particles}}{\text{cm}^2 \cdot \text{history}}\right) \cdot \left(\frac{\text{histories}}{\text{sec}}\right) \cdot (\text{b}) \cdot \left(\frac{\text{MeV}}{\text{collision}}\right) \cdot \left(\frac{\text{atoms}}{\text{b} \cdot \text{cm}}\right) \cdot \left(\frac{\text{cm}^3}{\text{g}}\right) = \left(\frac{\text{MeV}}{\text{g} \cdot \text{sec}}\right)$$

The energy absorbed may be converted to Roentgen (R) if air is the absorbing material. The energy absorbed may be divided by the energy required to produce an ion pair in air (W) to convert to charge deposited. The charge deposited may be multiplied by the definition of a Roentgen to convert to exposure in units of Roentgen. The time unit may also be converted to the more conventional hours. The value for W and R were taken from Table 1.

$$T \cdot WGT \cdot \sigma_t \cdot \sigma_h \cdot \left(\frac{\rho_a}{\rho_m \cdot W}\right) = \frac{\left(\frac{\text{MeV}}{\text{g} \cdot \text{sec}}\right) \cdot \left(\frac{\text{cm}^2}{\text{b}}\right) \cdot \left(\frac{\text{e}}{33.8\ \text{eV}}\right) \cdot \left(\frac{10^6\ \text{eV}}{\text{MeV}}\right) \cdot \left(\frac{1.602176487 \cdot 10^{-19}\ \text{C}}{\text{e}}\right)}{\left(\frac{\text{R}}{2.58 \cdot 10^{-4}\ \text{C/kg}}\right) \cdot \left(\frac{1000\ \text{g}}{\text{kg}}\right) \cdot \left(\frac{3600\ \text{sec}}{\text{hr}}\right)} = \frac{\text{R}}{\text{hr}}$$

In the above equation, T is calculated by MCNP, WGT is supplied in the SDEF card, and the cross-sections are applied using the -5 and -6 reactions on the FM card. Therefore, the tallies calculated by MCNP with an FM card constant of 1 are in the following units.

$$T \cdot WGT \cdot \sigma_t \cdot \sigma_h = \left(\frac{\text{particles}}{\text{cm}^2 \cdot \text{history}}\right) \cdot \left(\frac{\text{histories}}{\text{sec}}\right) \cdot (\text{b}) \cdot \left(\frac{\text{MeV}}{\text{collision}}\right) = \left(\frac{\text{MeV}}{\text{sec}}\right) \cdot \left(\frac{\text{b}}{\text{cm}^2}\right)$$

The remaining quantities constitute the constant C needed for the FM card to complete the conversion to

Roentgen per hour.

$$C = \frac{\rho_a}{\rho_m \cdot W}$$

The quantity ($\rho_m/\rho_a$) is simply the Avogadro constant divided by the formula mass of the material in question and converted to the appropriate units. The formula mass of the material may be calculated from the composition and density of the material, and the associated elemental masses. The formula mass calculation for air is shown in Table 10. The composition and density of air were taken from Section 3.6, and the elemental masses were taken from Table 3.

**Table 10. Formula Mass of Air**

| Air Composition | | Element Mass | Formula Mass |
|---|---|---|---|
| Element | Mass Fraction | (g/mol) | (g/mol) |
| C | 0.000124 | 12.010736 | 0.001489 |
| N | 0.755268 | 14.006743 | 10.578845 |
| O | 0.231781 | 15.999405 | 3.708358 |
| Ar | 0.012827 | 39.947677 | 0.512409 |
| Total | 1.000000 | | 14.801101 |

Since atom densities in MCNP stated are in units of atoms per barn centimeter, and mass densities in MCNP are stated in units of grams per cubic centimeter, the quantity ($\rho_a/\rho_m$) must be stated in units of square centimeters per barn gram and not simply inverse grams. The conversion factor necessary to calculate exposure in units of Roentgen per hour from a fluence tally is given by:

$$\frac{\rho_a}{\rho_m} = \left(\frac{6.02214179 \cdot 10^{23}\ \text{atoms}}{\text{mol}}\right) \cdot \left(\frac{\text{mol}}{14.80101\,\text{g}}\right) \cdot \left(\frac{10^{-24}\ \text{cm}^2}{\text{b}}\right) = 4.069 \cdot 10^{-2}\ \frac{\text{cm}^2}{\text{b} \cdot \text{g}}$$

$$C = \frac{\left(4.069 \cdot 10^{-2}\ \frac{\text{cm}^2}{\text{b} \cdot \text{g}}\right) \cdot \left(\frac{1000\,\text{g}}{\text{kg}}\right) \cdot \left(\frac{\text{e}}{33.8\,\text{eV}}\right) \cdot \left(\frac{10^6\,\text{eV}}{\text{MeV}}\right)}{\left(\frac{1.602176487 \cdot 10^{-19}\ \text{C}}{\text{e}}\right) \cdot \left(\frac{\text{R}}{2.58 \cdot 10^{-4}\ \text{C/kg}}\right) \cdot \left(\frac{3600\,\text{sec}}{\text{hr}}\right)} = 2.691 \cdot 10^{-6} \left(\frac{\text{sec}}{\text{MeV}}\right) \cdot \left(\frac{\text{cm}^2}{\text{b}}\right) \cdot \left(\frac{\text{R}}{\text{hr}}\right)$$

This factor was applied to all tallies using the FM card, along with the absorption cross-section (-5) and heating cross-section (-6).

## 3.8 MCNP Models

A separate MCNP model was developed for each penetrometer listed in Table 4, except for the HHU penetrometers for the reasons stated in Section 3.3. Each MCNP model included a conically tipped carbon steel penetrometer filled with air and surrounded by a column of soil, and was designed to include the entire penetrometer. The soil column was modeled as a 4 foot by 4 foot square in cross-section and extending along the entire length of the penetrometer. The excavation site at the open end of the

penetrometer was not modeled. A sketch of a typical MCNP model is shown in Figure 2.

**Figure 2. MCNP Model**

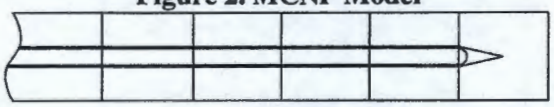

The radioactive material in the soil column was assumed to be a 1 foot by 1 foot square in cross-section, centered on the penetrometer, and divided into 1 foot sections along the length of the penetrometer. A separate source distribution was constructed for each cube. The source cubes started at the 50 foot mark to coincide with the start of the exposure rate measurements. Each source cube contains one curie of Cs-137/Sr-90 mixture in the same ratio as the FRG spill (883/1271=0.695 Ci C-137, 388/1271 = 0.305 Ci Sr-90).

Point detector tallies were positioned along the centerline of the instrument housing at the location of each exposure rate measurement. The exposure rate measurement points were generally positioned at the center of a source cube, although in many cases exposure rates were also measured in between the standard 1 foot increments. The point detector tally results were binned by the source distribution number using the SCX card to separate out the contribution to each exposure rate point from each source cube.

The MCNP files were executed to calculate the required factors relating activities in the source volumes and dose rates at the tally locations. All MCNP runs were performed by URS Princeton using validated code and computers. The MCNP output files are included as Attachment C.

### 3.9 Solvers

The results from each MCNP model were entered into a separate Microsoft Excel workbook, along with a vector of assumed source cube activities. A matrix equation was then entered to calculate the exposure rate at each point predicted by the assumed source cube activities. The measured exposure rates from Attachment A were entered alongside the calculated exposure rates, and the relative errors between the calculated and measured exposure rates were calculated and summed to form a metric representing the quality of the assumed solution.

Once the Excel workbooks were constructed, the solver built into the Analysis ToolPak was used to iteratively adjust the assumed activities to minimize the quality metric. The solver was first set to use the Adaptive option to obtain a rough solution. Subsequent solver runs then utilized the GRG Non-Linear option to polish the solution. It was often necessary to run the solver several times before the metric stopped changing. Occasionally some of the source activities were adjusted by hand to assist the solver in converging to a solution.

In general, it was possible to match the measured exposure rate curves quite closely despite the relatively coarse 1 foot spatial pitch of the MCNP models, with the total relative exposure rate error below 15% in most cases. The total calculated activities by penetrometer are listed in Table 11, along with the solution quality metrics. The activities of the individual 1-foot cubic source volumes are listed in Attachment D.

**Table 11: Penetrometer Activities**

| Cap ID | Activity (Ci) | Solution Quality |
|---|---|---|
| C8207 | 2.414E+03 | 10.27% |
| C8208 | 1.206E+03 | 12.22% |
| C8209 | 1.724E+02 | 2.28% |
| C8210 | 2.998E+03 | 21.44% |
| C8211 | 4.240E+03 | 2.61% |
| C8212 | 1.405E+01 | 7.64% |
| C8213 | 5.019E+01 | 13.93% |
| C8214 | 1.643E+03 | 8.54% |
| C9433 | 1.332E+02 | 14.89% |
| C9434 | 3.091E+03 | 10.11% |
| C9435 | 2.021E+03 | 11.38% |
| C9436 | 1.252E+03 | 17.10% |
| C9437 | 9.102E-05 | 1.88% |
| C9438 | 5.392E+03 | 19.24% |
| Total | 2.463E+04 | |

The activities obtained as part of this calculation were compared to the results in 0300X-CA-N0140 Revision 1 (WCH 2011). The details of the comparison are shown in Table 12.

**Table 12: Penetrometer Activity Comparison**

| Cap ID | Activity (Ci) | | Delta |
|---|---|---|---|
| | Rev 2 | Rev 1 | |
| C8207 | 2.414E+03 | 2.759E+03 | -14.32% |
| C8208 | 1.206E+03 | 8.195E+02 | 32.07% |
| C8209 | 1.724E+02 | 2.346E+02 | -36.08% |
| C8210 | 2.998E+03 | 2.107E+03 | 29.72% |
| C8211 | 4.240E+03 | 4.114E+03 | 2.97% |
| C8212 | 1.405E+01 | 1.893E+01 | -34.78% |
| C8213 | 5.019E+01 | 3.994E+01 | 20.43% |
| C8214 | 1.643E+03 | 1.112E+03 | 32.33% |

The measured and calculated exposure rate profiles may also be plotted against each other to visually evaluate the quality of the solutions. Solver results are shown graphically in Figure 3.

**Figure 3: Solution Quality**

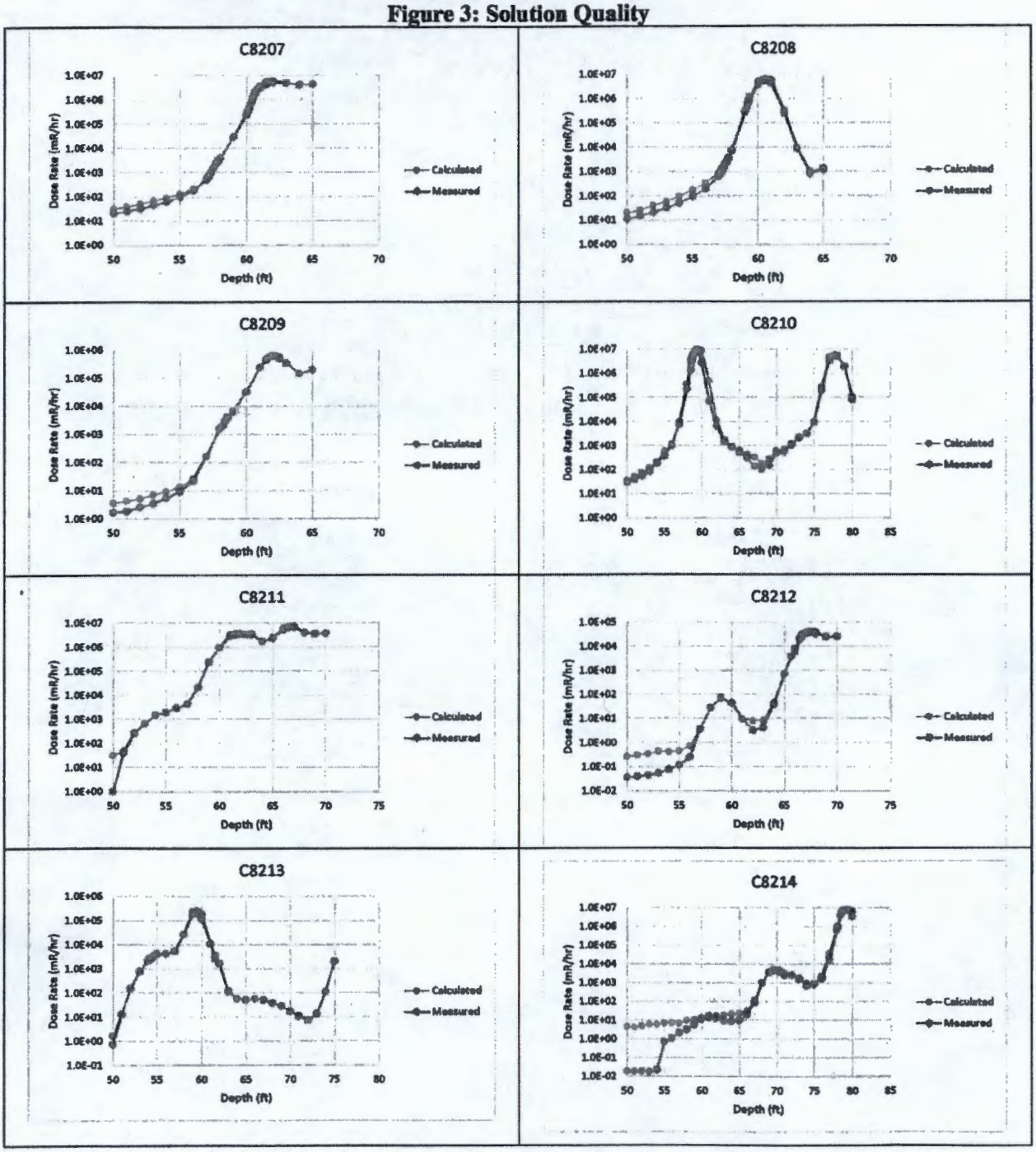

**Figure 3: Solution Quality**

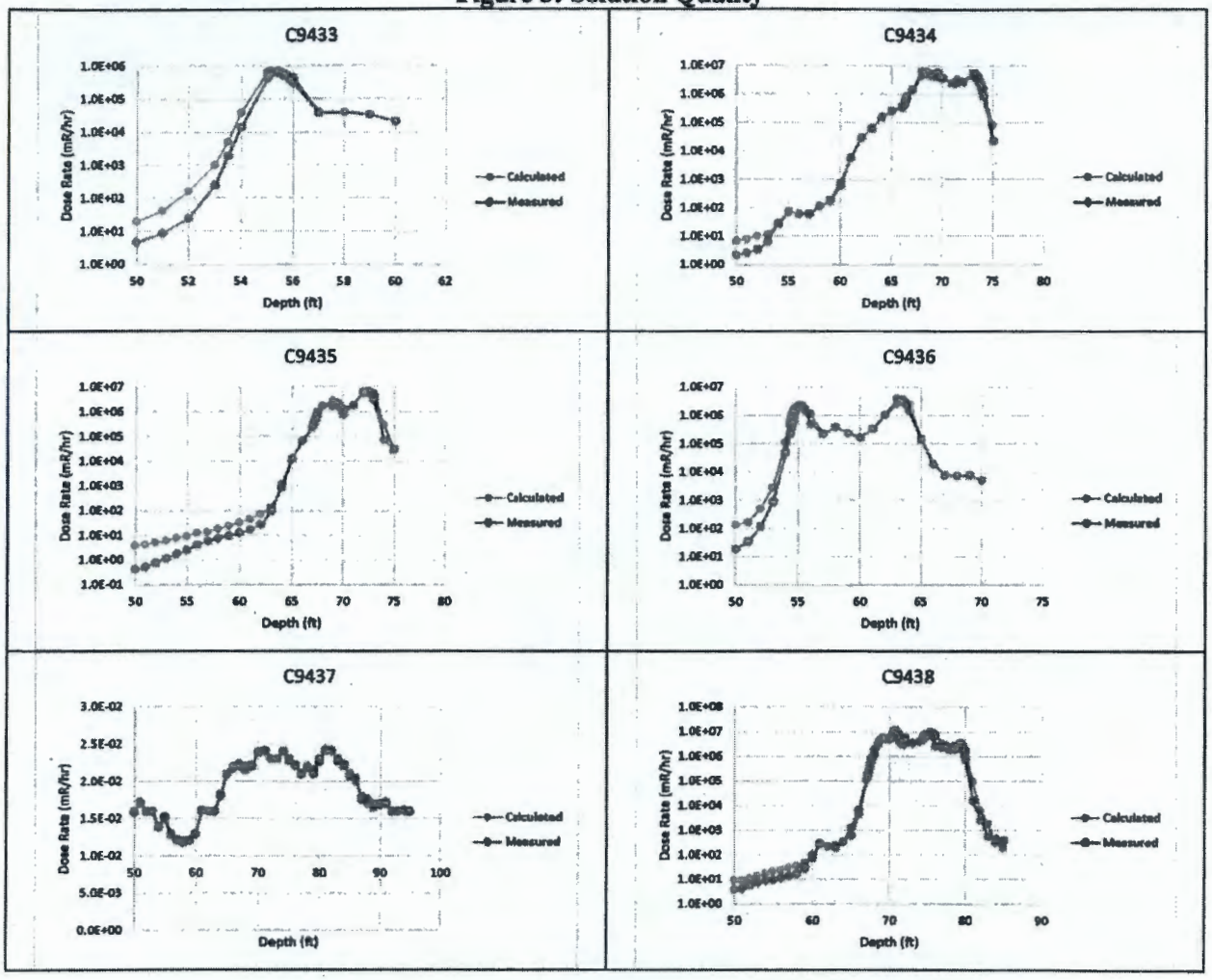

## 4.0 Contamination Plume Calculations

The activity distribution and total activity associated with the contamination plume are calculated in the following sections.

### 4.1 Activity Distribution

A histogram of the individual source cube activities was generated to determine the associated probability distribution. The histogram indicates that the soil activities actually consist of 3 separate populations, each with a log-normal distribution having a characteristic mean and standard deviation. Therefore, the soil contamination plume was modeled as having a profile consisting of low, mid, and high contamination zones. The source activity histogram and log-normal distributions are shown in Figure 4.

**Figure 4. Activity Distributions**

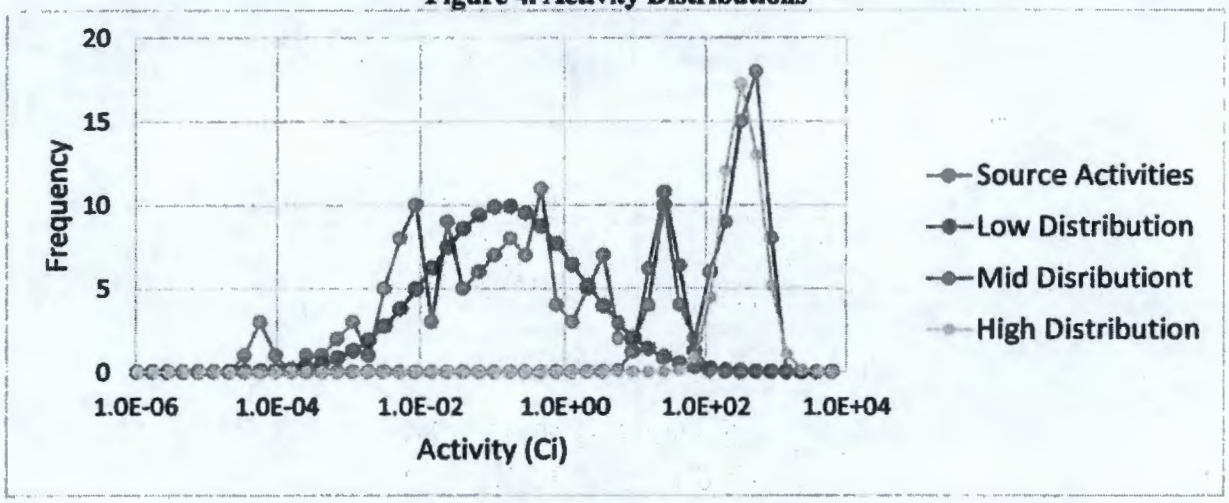


The three populations were constructed by defining activity cutoffs used to assign each source activity to one population. Cutoffs between the zones were set based on an inspection of the histogram. Population statistics for the source activities are shown in Table 13.

**Table 13: Population Statistics**

| Zone | Range (Ci) | Count | Mean (Ci) | Std Deviation |
|---|---|---|---|---|
| High | 100 - 1000 | 54 | 4.382E+02 | 4.005E+02 |
| Mid | 5 - 100 | 26 | 3.264E+01 | 2.488E+01 |
| Low | 0 - 5 | 118 | 4.574E-01 | 1.417E+00 |

## 4.2 Activity Profile

The penetrometer activities may be extended to approximate the activity profile beneath 324 B Cell as a whole. As discussed in Section 4.1, the activity profile consists of high, mid, and low contamination zones. Based on the penetrometer results, the contamination zones were assumed to extend uniformly around the expansion joint in the B Cell floor, spread vertically, and to end at the cobble layer.

The assumption of uniform contamination around the expansion joint is conservative since the survey results show that portions of the soil below the expansion joint are less heavily contaminated than others. The assumption that the contamination ends at the cobble layer is also reasonable since the hydraulic hammer unit penetrometers show that the level of contamination below the cobble layer is negligible compared to the level of contamination immediately below B Cell.

The approximate activity profile is shown in Figure 5.

**Figure 5. Activity Profile**

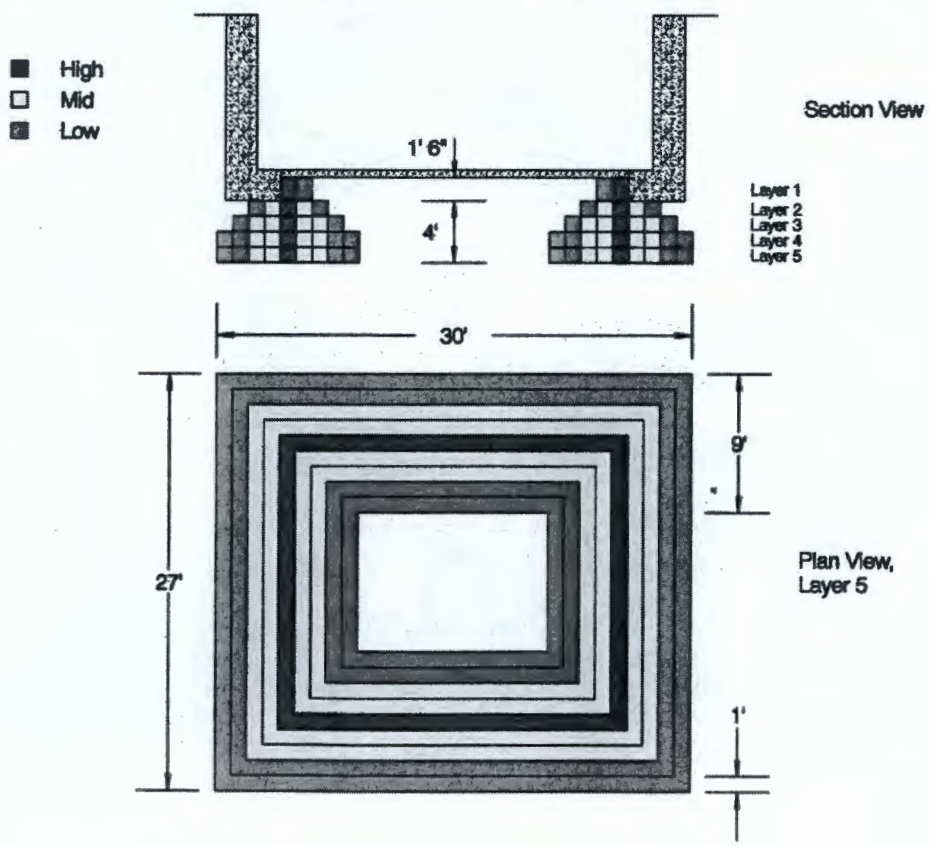

### 4.3 Total Activity

The surface areas of each zone were calculated using the dimensions in Figure 5, summed by layer, and multiplied by the layer thickness to determine the zone volumes per layer. The zone volumes per layer were then summed over the layers to calculate total zone volumes. The volumes of the different zones are shown in Table 14.

**Table 14. Contamination Zone Volumes**

| Layer | High ($ft^3$) | Mid ($ft^3$) | Low ($ft^3$) |
|---|---|---|---|
| Layer 1 | 117 | | 105 |
| Layer 2 | 78 | 156 | 156 |
| Layer 3 | 78 | 312 | 156 |
| Layer 4 | 78 | 312 | 312 |
| Layer 5 | 78 | 312 | 312 |
| Total | 429 | 1092 | 1041 |

Multiplying the zone concentrations in Table 13 by the zone volumes in Table 14 yields the total activity beneath 324 B Cell. The total activity was then split into Cs-137 and Sr-90 activities using the activity ratio present in the FRG Canister Fabrication project spill. The total activity calculations are summarized in Table 15.

**Table 15. Contaminated Soil Activities**

| Zone | Volume ($ft^3$) | Soil Contamination ($Ci/ft^3$) | Cs-137 Activity (Ci) | Sr-90 Activity (Ci) | Zone Activity (Ci) |
|---|---|---|---|---|---|
| High | 429 | 4.382E+02 | 1.306E+05 | 5.739E+04 | 1.880E+05 |
| Mid | 1092 | 3.264E+01 | 2.476E+04 | 1.088E+04 | 3.564E+04 |
| Low | 1041 | 4.574E-01 | 3.308E+02 | 1.454E+02 | 4.761E+02 |
| Total | 2562 | | 1.557E+05 | 6.842E+04 | 2.241E+05 |

The total activity of 224 kCi in Table 15 represents a 40% increase over 0300X-CA-N0140 Revision 1 (WCH 2011).

### 4.4 Actinide Activity

The sources of Cs-137 and Sr-90 used in the FRG glass log project both contained residual quantities of actinides that caused the logs to be considered transuranic (TRU). Glass samples from four logs obtained during manufacture were analyzed for Sr-90 and Pu-239/240 content. The maximum ratio obtained was 0.81 μCi Pu-239/240 per Ci Sr-90 (BWHC 1997). The actinide content in the 300-296 waste site was calculated by applying the same Pu-239/240 to Sr-90 activity ratio to all three zones. The plutonium activity calculations are summarized in Table 16.

**Table 16. Plutonium Activities**

| Zone | Sr-90 Activity (Ci) | Pu-239/240 To Sr-90 Ratio | Pu-239/240 Activity (Ci) | Soil Density (g/mL) | TRU Concentration (nCi/g) |
|---|---|---|---|---|---|
| High | 5.739E+04 | 8.10E-07 | 4.649E-02 | 1.670E+00 | 2.291E+00 |
| Mid | 1.088E+04 | 8.10E-07 | 8.813E-03 | 1.670E+00 | 1.707E-01 |
| Low | 1.454E+02 | 8.10E-07 | 1.177E-04 | 1.670E+00 | 2.392E-03 |
| Average | 6.842E+04 | 8.10E-07 | 5.542E-02 | 1.670E+00 | 4.574E-01 |

The average soil in Table 16 has a Pu-239/240 concentration of slightly less than 0.5 nCi per gram, which is a factor of 200 below the transuranic waste limit of 100 nCi per gram. The most heavily contaminated soils have a Pu-239/240 concentration of slightly less than 2.5 nCi per gram, which is a factor of 40 below the transuranic waste limit.

The addition of other plutonium isotopes and Am-241 to this calculation would increase the TRU content, but the contribution from Pu-239 and Pu-240 is sufficiently low that these additions would not result in any of the soil approaching the transuranic limit.

### 4.5 Decay Heat

The soil activities calculated in Table 15 would create substantial decay heat beneath 324 B Cell. To quantify the decay heat, the Cs-137 and Sr-90 activities in Table 15 were entered into Radcalc 4.1 cases. The equilibrium activity ratios from the Radcalc 4.1 nuclear database were used to calculate the activities of Y-90 and Ba-137m, which were also entered into the Radcalc 4.1 cases. The decay heat calculations are summarized in Table 17. Radcalc output files are included as Attachment E.

**Table 17. Decay Heat**

| Scenario | Total Heat (W) | Volumetric Heat ($W/ft^3$) |
|---|---|---|
| High Zone | 1.004E+03 | 2.340E+00 |
| Mid Zone | 1.903E+02 | 1.743E-01 |
| Low Zone | 2.544E+00 | 2.444E-03 |
| Average | 1.197E+03 | 4.672E-01 |

This quantity of decay heat is enough to result in measurably increased soil temperatures. Modeling the soil temperature field would be difficult due to uncertainties in the thermal properties of the soil and the lack of well-defined boundary conditions. However, for scoping purposes, the temperature rise across a sphere of soil with a fixed boundary temperature may be easily calculated. From any introductory heat transfer textbook, the temperature rise from the boundary to the center of a heat-generating sphere is given by:

$$\Delta T = \frac{q \cdot r_o}{3 \cdot k}$$

where:

$q$ = volumetric heat generation rate
$r_o$ = radius of the sphere
$k$ = thermal conductivity of soil

Using the volumetric heat generation rates in Table 17 with a 1 foot diameter sphere and a generic sandy soil conductivity from Arya 2001, the temperature differences are given by:

$$q := \begin{pmatrix} 2.34E{+}000 \\ 1.743E{-}001 \\ 2.444E{-}003 \\ 4.672E{-}001 \end{pmatrix} \cdot \frac{W}{ft^3} \qquad r_o := 6 \cdot in \qquad k := 0.3 \cdot \frac{W}{m^2 \cdot K} \qquad \frac{q \cdot r_o}{3 \cdot k} = \begin{pmatrix} 25.19 \\ 1.88 \\ 0.03 \\ 5.03 \end{pmatrix} F$$

Thus the most heavily contaminated soil should experience a temperature increase of up to 25 °F over six inches, while the average soil would have a temperature increase of up to 5 °F over six inches. However, the soil temperatures in the vicinity of the penetrometers will vary from this theoretical profile due to the action of the penetrometer.

### 4.6 Uncertainty Analysis

The methodology used in this calculation has three main sources of uncertainty.

- MCNP
- GRG Nonlinear Solver
- Contamination Zone Cutoffs

The probabilistic nature of MCNP calculations introduces uncertainties into each constant in the matrix equation used to convert measured dose rates into calculated activities. These uncertainties are generally less than 5% for the dose rate contributions closest to the associated source, but can be more significant with the dose rate contributions more distant from the source. These uncertainties limit the accuracy with which the model can reproduce the measured dose rates.

The GRG nonlinear solver is capable of solving almost any type of problem, but at the expense of universal convergence and uniqueness. As a result, for the same model, the solver may converge to a different solution depending on the initial conditions. The solver may also fail to converge if one or more adjustable parameters are in the vicinity of a local minimum.

The cutoffs used to separate the source activities into high, medium, and low zone populations are established at points in between the histogram peaks, but the particular cutoff point selected is somewhat subjective. It is estimated that the total uncertainty in the method is approximately ± 30%.